THE JOURNAL OF PHYSICAL CHEMISTRY A

Article

pubs.acs.org/JPCA

Intermolecular Interaction in the NH_3-H_2 and H_2O-H_2 Complexes by Molecular Beam Scattering Experiments: The Role of Charge Transfer

Fernando Pirani,[†] David Cappelletti,*[,†] Leonardo Belpassi,[‡] and Francesco Tarantelli*[,†,‡]

[†]Dipartimento di Chimica, Biologia e Biotecnologie, Università di Perugia, via elce di Sotto, 8, Perugia 06123, Italy

[‡]Istituto di Scienze e Tecnologie Molecolari del CNR (CNR-ISTM), via elce di Sotto, 8, Perugia 06123, Italy

ABSTRACT: New molecular beam scattering experiments are reported for the ammonia–hydrogen system recording with unprecedented resolution "glory" quantum interferences in the total cross sections. Direct comparison with the analogous water–hydrogen complex, investigated under the same experimental conditions, highlights relevant differences in the intermolecular interaction affecting the observables. Analysis of the electronic charge displacement accompanying formation of both complexes, calculated using very accurate ab initio methods, helps to rationalize the experimental findings and unveils the selective and crucial role of charge transfer in driving water interactions and formation of a weak hydrogen bond.

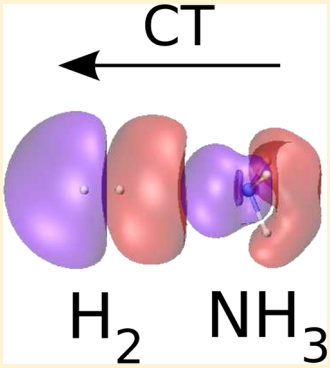

1. INTRODUCTION

The ammonia–hydrogen and water–hydrogen aggregates are among the simplest, prototypical examples of a noncovalent intermolecular bond between hydrogenated molecules. The intermolecular interactions which characterize these complexes have attracted a lot of attention, since they control relevant elementary (radiative and nonradiative) processes occurring in galaxies, interstellar clouds, and hydrogen-rich atmospheres of heavy planets. The dynamics of the gas-phase collisions of the species involved strongly depends on important features of the multidimensional intermolecular potential energy surfaces (PES), such as barriers, anisotropies, binding energy, and structure in the most stable configurations.[1−3] Moreover, detailed knowledge of the features of the PES, in particular, in the long-range region, and of the balance of the various interaction components is important to cast light on the origin, strength, and selectivity of the weak intermolecular hydrogen bond.[4−6] In particular, it is important to assess if ammonia, as observed for water,[3,7,8] may show in embryo a stereoselective Lewis acid–basic character when interacting with H_2. A large number of studies can be found in the literature (see, for instance, refs 1−3, 7, 9−16), providing information on H_2O-H_2 or NH_3-H_2, although detailed experimental characterizations are scarce. Herein, we propose for the first time a direct experimental comparison of these two prototype systems, carried out by molecular beam scattering under identical conditions. Experimental observations have been coupled with a detailed theoretical analysis based on the mapping of the electron density modification upon complex formation. Our efforts aim at discovering and explaining similarities and differences in the behavior of these two prototype weakly bound complexes, as determined by the nature of their intermolecular interaction.

Recently,[8] combination of new experimental and theoretical data allowed us to give a detailed characterization of the water–hydrogen binary interaction. We measured and analyzed the total integral cross section, Q, as a function of the collision velocity, v, via molecular beam experiments exploiting rotationally *hot* water molecules scattered in the thermal energy range. The measured *glory* quantum interference structure appeared clearly shifted with respect to predictions based on the usual well-established models of the noncovalent forces governing the interaction. This finding indicates the presence, at intermediate intermolecular distances, of an additional stabilizing interaction contribution which, with the help of accurate ab initio calculations and charge displacement analysis, could be clearly attributed to a charge-transfer (CT) component of about 2.5 meV per millielectron transferred. We could also observe that the pronounced stereospecificity of the CT contribution and its exponential decay with intermolecular distance control important features of the PES, such as the structure and energetics of some stable configurations.

This article reports analogous new molecular beam scattering experiments on ammonia–hydrogen carried out under high-resolution conditions and combined with new high-level ab initio calculations. Our investigation provides an accurate determination of the absolute scale of the rotationally averaged interaction and simultaneous characterization of the main features of the PES and the electronic charge density changes occurring upon formation of the complex. This yields quantitative information on the strength and relative role of the leading interaction components, in particular, of CT and its stereospecificity,

Received: August 16, 2013
Revised: October 29, 2013
Published: October 29, 2013

and permits an illuminating comparison between the water−hydrogen and ammonia−hydrogen systems investigated with identical techniques and experimental conditions. The next section summarizes basic aspects of the experimental technique and reports on the measured cross-section data and the obtained information on the intermolecuar interactions. Section 3 describes the charge displacement analysis and its relation with the experimental findings. Some conclusions follow in the final section.

2. EXPERIMENTAL RESULTS AND DATA ANALYSIS

Experiments have been carried out in a molecular beam (MB) apparatus which basically consists of a set of differentially pumped vacuum chambers where a MB is produced by gas expansion, collimated by two skimmers and one defining slit, velocity analyzed by a selector (six rotating slotted disks), attenuated by collisions with a target gas contained in a scattering chamber, and detected by a quadrupole mass spectrometer. All details on the apparatus and conditions used have been reported in previous papers.[8,17,18] Deuterated molecules (ND_3 and D_2) have been used instead of lighter NH_3 and H_2 to take advantage of the smaller background signal in the detector and of the better kinematic conditions, due to the reduction of random thermal motion of heavier target species. Moreover, as also discussed below, modifications of the molecular center of mass position due to isotopic changes provide negligible effects on the interaction measured under the present conditions.[8]

Measurements have been performed under two different experimental conditions, namely, by scattering ammonia projectiles by hydrogen targets or vice versa. Use of nearly effusive ammonia MB, containing randomly oriented, rotationally hot molecules, scattered by D_2 flowing in the scattering chamber kept at 90 K, permitted us to compare directly the obtained $Q(v)$ data with those measured under the same conditions for the water−hydrogen system (see Figure 1).

On the other hand, the scattering of D_2 projectiles by ND_3 targets, contained in the scattering chamber at room temperature, occurs under better velocity resolution conditions, since the random thermal motion of the target decreases by about 20%. These conditions are mandatory to fully resolve quantum interference effects in the velocity dependence of the cross section (see Figure 2).

It has been demonstrated[20] that, under the present experimental conditions, the interaction anisotropy and inelastic events play minor roles. The elastic cross section shows a dependence on the rotational state only for very low levels, i.e., those exhibiting a pronounced spatial quantization.[20] Indeed, such effects have been measured for scattering of supersonic cold molecular beams.[21] This effect vanishes for the higher rotational levels typical of thermal energy distributions such as those in the present experiment. Moreover, also the internal inversion motion of ammonia is expected not to affect the present observations.[22] It may consequently be assumed that the interaction effectively probed must essentially be the spherical average of the PES and can thus be represented by a simple radial potential.[17,20,22] We therefore carried out analysis of the experimental data using the improved Lennard−Jones (ILJ) potential model,[17,23] whose formulation exploits the balance of attractive and repulsive terms, both depending on the intermolecular distance r

$$V(r) = \varepsilon\left[\frac{6}{n(r)-6}\left(\frac{r_m}{r}\right)^{n(r)} - \frac{n(r)}{n(r)-6}\left(\frac{r_m}{r}\right)^{6}\right] \quad (1)$$

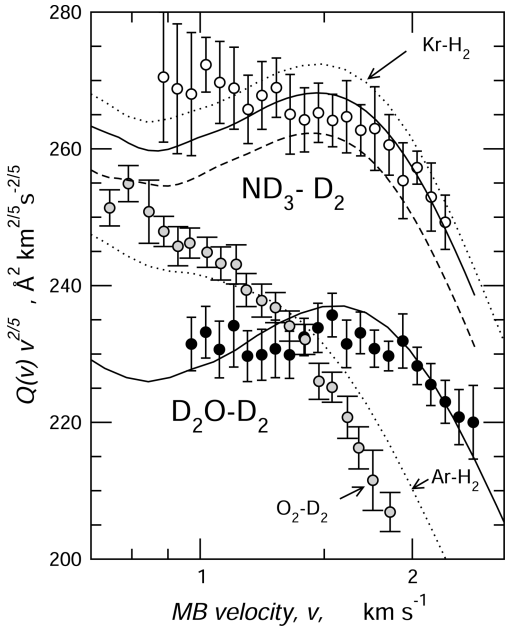

Figure 1. Experimental and calculated best-fit cross sections Q (solid lines) for ND_3−D_2 (open circles) and D_2O−D_2 (filled black circles) as a function of molecular beam velocity v. Data are plotted as $Q(v)v^{2/5}$ to emphasize the quantum interference oscillations.[23] Dashed line is the cross section resulting from a recent accurate ab initio NH_3−H_2 PES.[1] Also shown, for comparison, are the cross sections for Kr−H_2 and Ar−H_2 (dotted lines) calculated from accurate PES data[25,26] and the experimental cross section for the O_2−D_2 system (filled gray circles).[8] All calculated cross sections have been obtained in the center-of-mass frame using the JWKB method[19] and convoluted in the laboratory system for direct comparison with experimental data.[23]

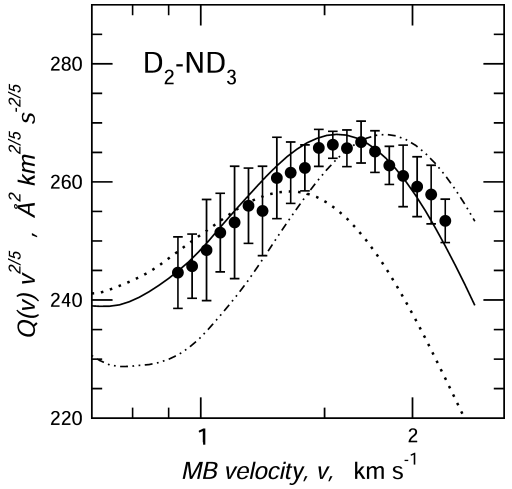

Figure 2. Experimental cross-section and calculated best-fit line (solid) for D_2−ND_3 as a function of MB velocity v. Dotted line and dotted−dashed line represent the cross section that would be obtained in the absence of CT energy stabilization (ε = 6.5 meV, r_m = 3.71 Å) and with an energy stabilization equal to that determined for water−H_2 (ε = 8.6 meV, r_m = 3.61 Å), respectively (see the text for details).

where

$$n(r) = \beta + 4\left(\frac{r}{r_m}\right)^2 \quad (2)$$

Parameters ε (depth of the potential well) and r_m (equilibrium distance) have been optimized in order to reproduce the

dx.doi.org/10.1021/jp408214p | J. Phys. Chem. A 2013, 117, 12601−12607

measured cross sections to within the calibration uncertainty (3−4%) of their absolute scale. As reported previously[17,23] we take $\beta = 9$, a value typical of weak intermolecular interactions between neutral species.[23] More details on the formulation and reliability of the ILJ potential function have been extensively discussed and tested elsewhere.[17,23,24]

Figures 1 and 2 report the measured $Q(v)$ and the corresponding fits. The magnitude of the cross section, mainly affected by the long-range attraction, directly depends on the $\varepsilon \times r_m^6$ product. Once this product has been determined on the basis of the ND_3-D_2 measurements, the values of the ε and r_m parameters have been best fitted to reproduce the well-resolved *glory* structure of the D_2-ND_3 cross section (Figure 2). Its noteworthy to remember that the *glory* quantum interference is controlled essentially by the potential well features.[23]

The final values are $\varepsilon = 7.35 \pm 0.30$ meV and $r_m = 3.70 \pm 0.06$ Å. As in previous cases,[23] the good fit of the experimental observables supports the validity of the present analysis and of the isotropic potential model. Figure 1 also shows the $Q(v)$ function calculated using the spherical average of a recent accurate PES[1] for which $\varepsilon = 7.20$ meV and $r_m = 3.64$ Å. Because the elastic cross-section is not sensitive to the details of the internal degrees of freedom of the colliding molecules, the isotopic effect has been estimated to be negligible,[2,8] and therefore, the comparison provides a further independent accuracy assessment. Moreover, our determined potential parameters are close to those obtained from differential cross sections.[13]

Data shown in Figure 1 are extremely revealing of the different features of the interaction in ammonia−hydrogen and water−hydrogen complexes. Compared to the water complex, the overall magnitude of the cross section is about 12% larger in the ammonia complex and the position of the glory maximum is shifted by about 4% at lower velocities. Although the fwhm of the velocity selector is better than 5%, the width of the relative velocity distributions, used in the center of mass laboratory frame transformation at each selected beam velocity, is much larger due to the D_2 thermal motion in the scattering chamber. Therefore, the mentioned 4% shift has been evaluated considering the cross sections in the center of mass system.

These findings emphasize that at long range the larger polarizability of ammonia (2.16 vs 1.47 Å^3 of water) causes stronger attraction toward H_2 (by about 34%), but at intermediate and shorter distances the global (attraction plus repulsion) interaction in ammonia−hydrogen is weaker than in water−hydrogen, resulting in a shallower potential well. We recall here that the best-fit ILJ parameters for the water complex are $\varepsilon = 8.20$ meV and $r_m = 3.45$ Å.[8] It is further quite illuminating to compare the D_2O-D_2 cross section with that of O_2-D_2 or $Ar-H_2$ and, at the same time, compare the cross section of ND_3-D_2 with that of $Kr-H_2$. The polarizabilities of O_2 (1.60 Å^3) and Ar (1.64 Å^3) are close to that of water, while the polarizability of Kr (2.49 Å^3) is similar to that of ammonia. Therefore, the corresponding complexes with the hydrogen molecule represent useful reference systems. For these reasons, in Figure 1 $Q(v)$ data are compared with measurements, obtained under the same experimental conditions, for O_2-D_2 ($\varepsilon = 5.90$ meV and $r_m = 3.63$ Å) and calculations performed using the $Ar-H_2$ ($\varepsilon = 6.29$ meV and $r_m = 3.59$ Å) and $Kr-H_2$ ($\varepsilon = 7.28$ meV and $r_m = 3.72$ Å) potentials accurately characterized by coupling spectroscopic and ab initio data.[25,26] While the average value of cross sections depending on the long-range attraction behaves as expected, a shift of the glory maximum of about 25% at higher velocity is exhibited by water−hydrogen with respect to both $Ar-H_2$ and O_2-H_2. As is well known,[19] a glory quantum interference pattern can shift at higher MB velocities only if the interaction energy around the turning point, i.e., in the proximity of the well depth, increases. Therefore, the experimental observation indicates clearly the presence of an extra stabilization energy[27] in the water complex (i.e., besides the expected dispersion and induction terms) of ∼2 meV as compared to the Ar and O_2 complexes.[8] By contrast, ammonia−hydrogen and $Kr-H_2$ adducts show, within the experimental resolution, a very similar magnitude of the average cross sections and a glory maxima coincident, resulting in a nearly identical average interaction potential. These findings suggest that in the two isoelectronic systems the additional CT component plays a different role (much weaker in ammonia), determining a different interaction balancing at long and intermediate intermolecular distances, respectively. Moreover, for ammonia−hydrogen the stabilization contribution at the equilibrium distance should not exceed ∼1 meV. Such a value has been estimated as the difference between the present determinations and predictions of correlation formulas,[28,29] providing the depth of the potential well arising from the combination of size repulsion with dispersion and induction contributions ($\varepsilon = 6.5$ meV and $r_m = 3.71$ Å).

3. CHARGE DISPLACEMENT ANALYSIS

In order to offer a theoretical assessment of the present experimental findings, we carried out a detailed charge displacement (CD) study[6,8,31−34] of the electron density rearrangement accompanying NH_3-H_2 formation and compared the results to those obtained for water−H_2.[8] We recall here that the object of CD analysis is the function

$$\Delta q(z) = \int_{-\infty}^{z} dz' \int_{-\infty}^{\infty}\int_{-\infty}^{\infty} \Delta\rho(x, y, z')dx\, dy \qquad (3)$$

where $\Delta\rho$ is the electron density difference between the complex and its separated fragments (at the same positions) and z is any chosen axis joining them. $\Delta q(z)$ gives at each point along z the amount of electronic charge that, upon formation of the complex, is transferred from the right to the left side of the perpendicular plane through z. z is chosen here as the line joining the center of mass (c.m.) of the two molecules.[37] Electron densities have been computed at the coupled-cluster level of theory[35] with single and double excitations (CCSD) using the aug-cc-pVQZ basis set,[36] which ensures fully reliable convergence of the CD function. Analysis of $\Delta q(z)$ may be very helpful for qualitative assessment of the presence and extent of even small amounts of CT. CT may be confidently said to take place when $\Delta q(z)$ is appreciably different from zero and does not change sign in the region between the fragments. In this case it may be comparatively estimated by taking the CD function value at a point between the fragments. We have usually chosen[6] to separate the fragments and extract the CT value at the so-called isodensity boundary, i.e., the point along z where the electron densities of the noninteracting fragments become equal. We often noticed that this point turns out to be close to the minimum of the total molecular density between the fragments and also close to the bond critical point[30] when there is one.

In Figure 3 we compare the density change contour plots and CD functions for NH_3-H_2 and H_2O-H_2 in two geometry arrangements which exemplify typical and opposite charge-transfer patterns. In the upper panels of the figure the two complexes are at their respective most stable geometry, in

dx.doi.org/10.1021/jp408214p | J. Phys. Chem. A 2013, 117, 12601−12607

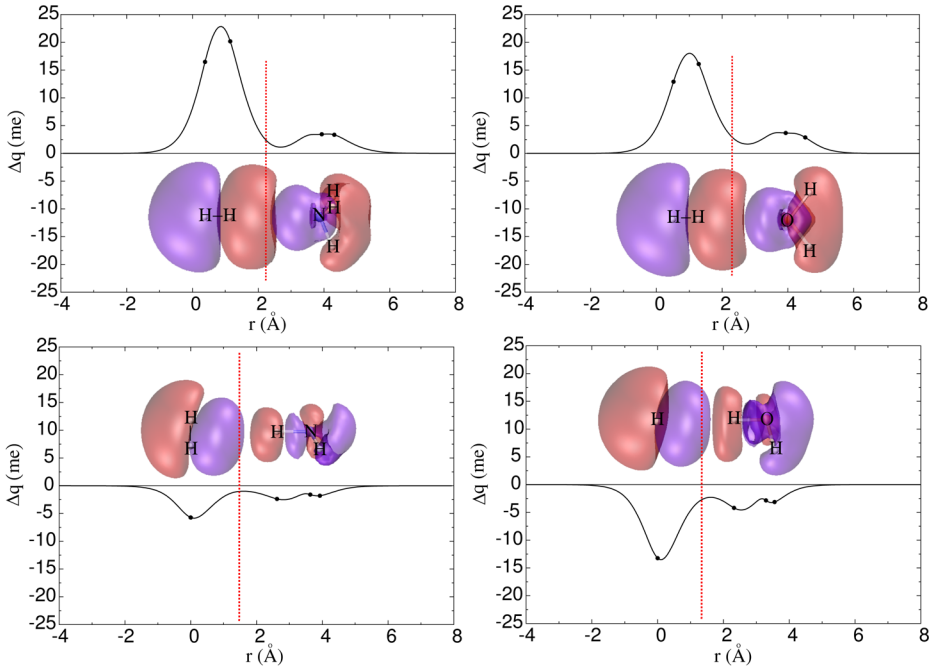

Figure 3. Charge displacement curves and density difference contour plots describing formation of H_2–NH_3 (left) and H_2–H_2O (right). Upper panels show complexes at their most stable nuclear configuration, while in the lower panels H_2 approaches the partner molecule from the opposite side, i.e., along a O–H or N–H bond. Isodensity surfaces are for $\Delta\rho = \pm 0.03$ me/bohr^3 (negative value in red, positive in blue). Dots on the CD curves correspond to the projection on the z axis of the atom positions. Vertical dashed lines mark the isodensity boundaries between the fragments. Note that the hydrogen molecule in the lower right panel is perpendicular to the plane of the figure.

which H_2 lies along the symmetry axis of the partner molecule, on the nitrogen and oxygen side, respectively. The pattern of electron displacement is clearly very similar, both qualitatively and quantitatively, in both complexes. As should be expected, the H_2 electron cloud is strongly polarized by the hydride induction, with density shifting from the region around the hydrogen closer to ammonia (water) toward the far hydrogen atom. The density depletion around the former hydrogen is shown by the red lobe in the contour plot and the corresponding negative slope of the CD curve. Density accumulation at the far hydrogen is indicated by the blue density difference lobe and the positive CD slope. CD curves evidence that H_2 polarization is more pronounced in the ammonia than in the water complex, with the curves reaching a maximum of about 23 and 18 me, respectively, near the H_2 midpoint. A small overall polarization is also seen in the ammonia and water regions. The CD curve is in both cases positive across the whole complex, proving that at each point along the axis some amount of electronic charge has moved in the direction from the hydride toward H_2. In the region between the molecules the curves are relatively flat and we notice that, in contrast with H_2 polarization, the water curve is slightly more positive than the ammonia one, indicating a correspondingly larger CT from water to H_2. Taking the isodensity boundary as our reference, CT to hydrogen is 2.41 me in the ammonia case and 2.85 me in the water one. Extensive characterization of the polarization and CT zones of the CD curve is beyond the purposes of the present work and presented in ref 6.

In the lower panels of the figure H_2 is on the opposite side of the partner molecule, with its c.m. lying on a N–H (O–H) axis. The other relative coordinates are fully optimized. Note that in the water case the H_2 bond lies perpendicular to the water plane, while in the ammonia complex it lies on the ammonia symmetry plane. Here we see a completely different CD pattern, with CD curves negative everywhere, i.e., electrons flowing away from H_2 and toward the other molecule. However, what is most important here is that the density perturbation is everywhere small in the ammonia case and substantially more pronounced in the water complex. As a result, CT from H_2 to ammonia, measured at the isodensity boundary, is only 1.0 me, while it is almost three times larger (2.8 me) and similar (in magnitude) to the upper-panel arrangement in the water case.

The scenario exemplified by Figure 3 is general: we find that a CT component of the interaction is present in both the water and the ammonia complexes with H_2, but while this component is of comparable magnitude in the nuclear orientations where the hydride molecule is the electron donor, it is very different in the configurations where the hydride is the acceptor (proton donor). Here, remarkably, CT persists just as significant in the water complex, while it becomes much smaller in the ammonia case. We are thus led to conclude that, when averaged over all possible orientations, the CT component plays an overall more significant role in stabilizing the water complex than the ammonia one.

An insightful confirmation of this picture is provided in Figure 4. Herein, a comparison of the trends in interaction energy and CT magnitude (taken at the isodensity boundary) along a representative PES section covering the main aspects discussed and corresponding to H_2 circling around either ammonia or water, with its c.m. lying on the water plane and on a ammonia symmetry plane, respectively, is presented. At each angle of revolution the other geometry parameters are relaxed. The angle in question, ϕ, is that between the hydride symmetry axis and the axis joining the c.m. of the two molecules, with $\phi = 0$ corresponding to H_2 on the hydrogen side. In the ammonia case, the two half circles traveled by H_2 below and above $\phi = 180°$ are not exactly equivalent (though similar) and only the first one, where H_2 passes in front of a hydrogen atom

dx.doi.org/10.1021/jp408214p | J. Phys. Chem. A 2013, 117, 12601–12607

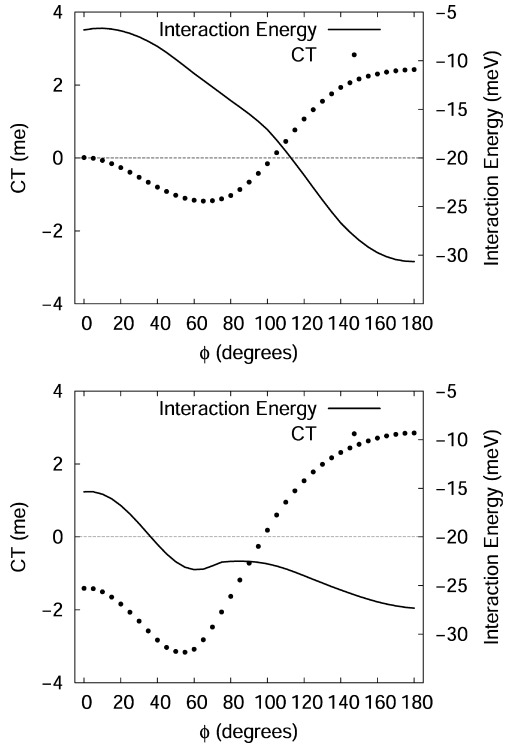

Figure 4. CT values at the isodensity boundary (dots) for different orientations of NH_3–H_2 (top) and H_2O–H_2 (bottom). Corresponding interaction energy curve (solid lines) is also shown (see text). Positive CT is from ammonia (water) to H_2 and negative from H_2 to ammonia (water).

(for which CT is more pronounced and a stricter comparison with water–H_2 can be made), is shown in the figure. As one can see, CT varies significantly along the path, displaying a strong anisotropy in both complexes, but a significantly wider oscillation is present in the water case. The pattern of CT is surprisingly similar in both complexes for ϕ above ~120°, where ammonia and water act as electron donors (CT is positive). At ϕ = 180°, in correspondence with a CT maximum, the global minimum of the PES is found. Note that this is deeper in the ammonia case, in contrast with the experimentally determined spherical average. For smaller angles, where CT is negative, i.e., H_2 is the electron donor, a maximum of CT magnitude is also found at ϕ values corresponding to the H_2 c.m. pointing almost directly toward one O–H (N–H) bond. However, while in the water complex this maximum is sharper and even larger (3.1 me) than the ϕ = 180° one, it is much less pronounced in the ammonia case. It is indeed eye catching that, in essentially exact coincidence with this CT peak, a secondary minimum of the water–H_2 PES is found, whereas the reduced electron-acceptor character of ammonia prevents formation of an analogous minimum, and only a weak change of curvature in the energy curve at ϕ ~70° is observed instead.

The relative role of CT in the experimentally observed intermolecular potential which, we recall, is averaged over all possible orientations and thus displays only radial dependence, can be further aptly assessed by studying the dependence of CT on distance. To this end, using CD analysis, we calculated CT (at the isodensity boundary) on a grid of angles and intermolecular distances r, in analogy to our previous investigation of water–H_2.[8] The CT magnitude turns out to be very accurately modeled as CT = be^{-ar}, where the parameter a, as previously also found,[8] is almost independent of orientation and b (which is independent of r) is easily averaged over the various orientations explored. We further calculated separate averages for the orientations where H_2 is the electron donor or acceptor, and the final results for both water–H_2 and ammonia–H_2 are displayed in Figure 5. The figure illustrates clearly the smaller

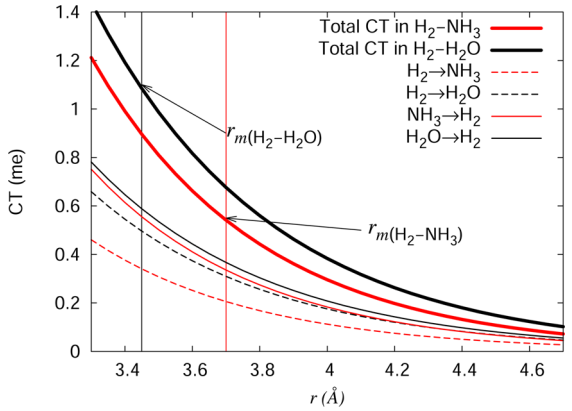

Figure 5. Computed radial dependence of the orientationally averaged CT magnitude in H_2O–H_2 and NH_3–H_2. Separate curves are also shown for the CT components where H_2 is the electron donor and acceptor, respectively.

overall CT in the ammonia complex at all distances and also the fact that the difference between the two global CT curves is almost entirely due to the much smaller electron acceptor (proton donor) character of ammonia. The vertical lines in the figure mark the position of the respective minima of the radial potential, as determined experimentally. These help to visualize very clearly that in the region around the potential energy minimum the actual impact of CT on the water interaction with H_2 must be much larger than in the ammonia case, not only because of the intrinsically more pronounced hydrogen-bonding propensity of water but also because of the (partly consequent) significantly shorter distance of H_2 approach. Indeed, at the minimum of the potential well, CT in the water complex (~1.1 me) is almost exactly twice that in the ammonia complex. The larger interaction energy at the global minimum of NH_3–H_2 compared to the water complex signals that, at other configurations, the interaction must on the contrary be weaker in order to produce the experimentally measured shallower average well depth.

Finally, we may very roughly estimate the energy stabilization associated with this CT using the conversion rate of ~2.5 eV/e, which we previously found useful in a series of similar complexes.[6,8] The resulting figures match comfortingly well the experimental estimates discussed earlier, lending further support to our analysis.

4. CONCLUSIONS

Understanding at the molecular level the interactions involving water, as well as other small hydrogenated molecules such as NH_3, is as important a scientific goal as it is elusive, with a potentially vast impact in fields ranging from astrophysics to biochemistry. Interesting case studies are represented by the H_2O–H_2 and NH_3–H_2 dimers. These molecular complexes are among the most fundamental in the visible universe, and detailed knowledge of their intermolecular interactions is vital for description of many phenomena, from interstellar masers to

dx.doi.org/10.1021/jp408214p | J. Phys. Chem. A 2013, 117, 12601–12607

hydrogen bonding. In this article we presented state-of-the-art molecular beam scattering experiments combined with an insightful charge displacement analysis in order to understand and bring into a useful perspective—amenable to modeling—the elusive and controversial subject of charge-transfer effects in the perturbative limit occurring in these weak intermolecular interactions.

The results presented here unambiguously show that, far from being typical van der Waals complexes, water and ammonia intermolecular interactions, even when very weak, possess a definite, strongly stereospecific, CT component, where water (or ammonia) may act as electron donor or acceptor depending on orientation. Careful comparison with the experimental results shows that the stabilization energy associated to CT is on the order of 2−3 eV per electron transferred but CT, especially in the hydrogen-bonding orientations, is much less pronounced for ammonia than for water. The reasons for such difference, as explained in the paper, are due to a subtle balance between long-range attractive and short-range repulsive terms in the overall intermolecular interaction.

A study of H_2S provides the next logical step in a systematic study of charge transfer in hydrogen bonding.

AUTHOR INFORMATION

Corresponding Authors

*E-mail: david.cappelletti@unipg.it.

*E-mail: franc@thch.unipg.it.

Notes

The authors declare no competing financial interest.

ACKNOWLEDGMENTS

This work was supported by the MIUR (PRIN 2010-2011 grant 2010ERFKXL).

REFERENCES

(1) Maret, S.; Faure, A.; Scifoni, E.; Weisenfeld, L. On the Robustness of the Ammonia Thermometer. *Mon. Not. R. Astron. Soc.* **2009**, *399*, 425−431.

(2) Weisenfeld, L.; Scifoni, E.; Faure, A.; Roueff, E. Collisional Excitation of Doubly Deuterated Ammonia ND_2H by Para-H_2. *Mon. Not. R. Astron. Soc.* **2011**, *413*, 509−513.

(3) Valiron, P.; Vernli, M.; Faure, A.; Wiesenfeld, L.; Rist, C.; Kedzuch, S.; Nola, J. R12-Calibrated H_2OH_2 Interaction: Full Dimensional and Vibrationally Averaged Potential Energy Surfaces. *J. Chem. Phys.* **2008**, *129*, 134306.

(4) Arunan, E.; Desiraju, G.; Klein, R.; Sadlej, J.; Scheiner, S.; Alkorta, I.; Clary, D.; Crabtree, R.; Dannenberg, J.; Hobza, P.; et al. Definition of the Hydrogen Bond (IUPAC Recommendations 2011). *Pure Appl. Chem.* **2011**, *83*, 1637−1641.

(5) Desiraju, G.; Steiner, T. *The Weak Hydrogen Bond in Structural Chemistry and Biology*; Oxford University Press: Oxford, U.K., 1999.

(6) Cappelletti, D.; Ronca, E.; Belpassi, L.; Tarantelli, F.; Pirani, F. Revealing Charge-Transfer Effects in Gas-Phase Water Chemistry. *Acc. Chem. Res.* **2012**, *45*, 1571−1580.

(7) Weida, M. J.; Nesbitt, D. High-Resolution Diode Laser Study of H_2H_2O van der Waals Complexes: H_2O as Proton Acceptor and the Role of Large Amplitude Motion. *J. Chem. Phys.* **1999**, *110*, 156−167.

(8) Belpassi, L.; Reca, M. L.; Tarantelli, F.; Roncaratti, L. F.; Pirani, F.; Cappelletti, D.; Faure, A.; Scribano, Y. Charge-Transfer Energy in the Water-Hydrogen Molecular Aggregate Revealed by Molecular-Beam Scattering Experiments, Charge Displacement Analysis, and ab Initio Calculations. *J. Am. Chem. Soc.* **2010**, *132*, 13046−13058.

(9) Jacox, M. E.; Thompson, W. E. Infrared Absorptions of $NH_3(H_2)$ Complexes Trapped in Solid Neon. *J. Chem. Phys.* **2006**, *124* (204304), 1−11.

(10) Danby, G.; Flower, D. R.; Valiron, P.; Schilke, P.; Walmsley, C. M. A Recalibration of the Interstellar Ammonia Thermometer. *Mon. Not. R. Astron. Soc.* **1988**, *235*, 229−238.

(11) Fabris, A. R.; Oka, T. Observation of $k = \pm 3$ Transitions in NH_3-H_2 Collisions. *J. Chem. Phys.* **1972**, *56*, 3168−3169.

(12) Abel, B.; Coy, S. L.; Klaassen, J. J.; Steinfeld, J. I. StatetoState Rotational EnergyTransfer Measurements in the $v^2 = 1$ State of Ammonia by InfraredInfrared Double Resonance. *J. Chem. Phys.* **1992**, *96*, 8236−8250.

(13) Bickes, R. W., Jr.; Duquette, G.; van den Meijdenberg, C. J. N.; Rulis, A. M.; Smith, K. M.; Scoles, G. Molecular Beam Scattering Experiments with Polar Molecules. *J. Phys. B* **1975**, *8*, 3034−3043.

(14) Ebel, G.; Krohne, R.; Meyer, H.; Buck, U.; Schinke, R.; Seelemann, T.; Andresen, P.; Schleipen, J.; ter Meulen, J. J.; Dierksen, G. H. F. Rotationally Inelastic Scattering of NH_3 with H_2: Molecular Beam Experiments and Quantum Calculations. *J. Chem. Phys.* **1990**, *93*, 6419−6432.

(15) Schleipen, J.; ter Meulen, J. J.; Offer, A. R. State-to-State Cross Sections for Rotational Excitation of Ortho- and Para-NH_3 by Ortho- and Para-H_2. Experiment Versus Theory. *Chem. Phys.* **1993**, *171*, 347−362.

(16) Willey, D. R.; Timlin, R. T., Jr; Deramo, M.; Pondillo, P. L.; Wesolek, D. M.; Wig, R. W. Pressure Broadening of NH_3 by H_2 From 15 to 40 K. *J. Chem. Phys.* **2000**, *113*, 611−615.

(17) Roncaratti, L. F.; Belpassi, L.; Cappelletti, D.; Pirani, F.; Tarantelli, F. Molecular-Beam Scattering Experiments and Theoretical Calculations Probing Charge Transfer in Weakly Bound Complexes of Water. *J. Phys. Chem. A* **2009**, *113*, 15223−15232.

(18) Pirani, F.; Bartolomei, M.; Aquilanti, V.; Scotoni, M.; Vescovi, M.; Ascenzi, D.; Bassi, D.; Cappelletti, D. Collisional Orientation of the Benzene Molecular Plane in Supersonic Seeded Expansions, Probed by Infrared Polarized Laser Absorption Spectroscopy and by Molecular Beam Scattering. *J. Chem. Phys.* **2003**, *119*, 265−276.

(19) Child, M. S. *Molecular collision Theory*; Academic Press: London, 1974.

(20) Aquilanti, V.; Ascenzi, D.; Cappelletti, D.; de Castro, M.; Pirani, F. Scattering of Aligned Molecules. The Potential Energy Surfaces for the Kr-O_2 and Xe-O_2 Systems. *J. Chem. Phys.* **1998**, *109*, 3898−3910.

(21) Aquilanti, V.; Ascenzi, D.; Cappelletti, D.; Franceschini, S.; Pirani, F. Scattering of Rotationally Aligned Oxygen Molecules and the Measurement of Anisotropies of van der Waals Forces. *Phys. Rev. Lett.* **1995**, *74*, 2929−2932.

(22) Pirani, F.; Roncaratti, L. F.; Belpassi, L.; Tarantelli, F.; Cappelletti, D. Molecular-Beam Study of the AmmoniaNoble Gas Systems: Characterization of the Isotropic Interaction and Insights into the Nature of the Intermolecular Potential. *J. Chem. Phys.* **2011**, *135*, 194301.

(23) Pirani, F.; Brizi, S.; Roncaratti, L. F.; Casavecchia, P.; Cappelletti, D.; Vecchiocattivi, F. Beyond the Lennard-Jones model: a Simple and Accurate Potential Function Probed by High Resolution Scattering Data Useful for Molecular Dynamics Simulations. *Phys. Chem. Chem. Phys.* **2008**, *10*, 5489−5503.

(24) Albertí, M.; Castro, A.; Laganá, A.; Pirani, F.; Porrini, M.; Cappelletti, D. Properties of an AtomBond Additive Representation of the Interaction for BenzeneArgon Clusters. *Chem. Phys. Lett.* **2004**, *392*, 514−520.

(25) Bissonnette, C.; Chuaqui, C. E.; Crowell, K. G.; Le Roy, R. J.; Wheatley, R.; Meath, W. J. A Reliable New Potential Energy Surface for H_2Ar. *J. Chem. Phys.* **1996**, *105*, 2639−2653.

(26) Wei, H.; Le Roy, R. J.; Wheatley, R. J.; Meath, W. J. A Reliable New Three-Dimensional Potential Energy Surface for H_2Kr. *J. Chem. Phys.* **2005**, *122*, 0843221.

(27) Aquilanti, V.; Cappelletti, D.; Pirani, F. Bond Stabilization by Charge Transfer: the Transition from Van der Waals Forces to the Simplest Chemical Bonds. *Chem. Phys. Lett.* **1997**, *271*, 216−222.

(28) Cambi, R.; Cappelletti, D.; Liuti, G.; Pirani, F. Generalized Correlations in Terms of Polarizability for Van der Waals Interaction Potential Parameter Calculations. *J. Chem. Phys.* **1991**, *95*, 1852−1861.

(29) Cappelletti, D.; Liuti, G.; Pirani, F. Generalization to Ion-Neutral Systems of the Polarizability Correlations for Interaction Potential Parameters. *Chem. Phys. Lett.* **1991**, *183*, 297−303.
(30) Bader, R. F. W. A Quantum Theory of Molecular Structure and its Applications. *Chem. Rev.* **1991**, *91*, 893−928.
(31) Belpassi, L.; Infante, I.; Tarantelli, F.; Visscher, L. The Chemical Bond between Au(I) and the Noble Gases. Comparative Study of NgAuF and $NgAu^+$ (Ng) Ar, Kr, Xe) by Density Functional and Coupled Cluster Methods. *J. Am. Chem. Soc.* **2008**, *130*, 1048.
(32) Belpassi, L.; Tarantelli, F.; Pirani, F.; Candori, P.; Cappelletti, D. Experimental and Theoretical Evidence of Charge Transfer in Weakly Bound Complexes of Water. *Phys. Chem. Chem. Phys.* **2009**, *11*, 9970.
(33) Cappelletti, D.; Candori, P.; Pirani, F.; Belpassi, L.; Tarantelli, F. Nature and Stability of Weak Halogen Bonds in the Gas Phase: Molecular Beam Scattering Experiments and Ab Initio Charge Displacement Calculations. *Cryst. Growth Des.* **2011**, *11*, 4279−4283.
(34) Bistoni, G.; Belpassi, L.; Tarantelli, F.; Pirani, F.; Cappelletti, D. Charge Displacement Analysis of the Interaction in the Ammonia Noble Gas Complexes. *J. Phys. Chem. A* **2011**, *115*, 14657−14666.
(35) Hampel, C.; Peterson, K. A.; Werner, H.-J. A Comparison of the Efficiency and Accuracy of the Quadratic Configuration Interaction (QCISD), Coupled Cluster (CCSD), and Brueckner Coupled Cluster (BCCD) Methods. *Chem. Phys. Lett.* **1992**, *190*, 1−12.
(36) Kendall, R. A.; Dunning, T. H.; Harrison, R. J. Electron Affinities of the FirstRow Atoms Revisited. Systematic Basis Sets and Wave Functions. *J. Chem. Phys.* **1992**, *96*, 6796−6806.
(37) This definition includes the change in density due to the antisymmetrization and renormalization of the total wave function made up from the nonorthogonal fragment wave functions.